Three-Dimensional Miscible Viscous Fingering in Porous Media

J.-C. Bacri, D. Salin, and R. Wouméni
Laboratoire d'Acoustique et Optique de la Matière Condensée, Université Pierre et Marie Curie, Tour 13, Boîte Postale 78, 4 place Jussieu, 75252 Paris CEDEX 05, France
(Received 17 June 1991)

Using an acoustic technique profile analysis we have studied the growth of viscous fingers inside 3D porous media. The experimental data support the definition of an instability parameter which captures the essential features of the viscous fingering; its dependence on the viscosity ratio, on the flow rate, and on the nature of the porous medium is compared to available theory. Our data demonstrate the predicted crossover between diffusive and linear growth and the growth enhancement due to coupling between large viscosity ratio and velocity-dependent hydrodynamic dispersion.

PACS numbers: 47.20.−k, 47.55.Mh, 68.10.Et

Viscous fingering [1–5] resulting from unstable fluid displacements in porous media has been studied extensively for forty years since the pioneering experiments of Hill. Most of the papers on viscous fingering deal with immiscible fluids, but indeed the problem involving miscible fluids deserves at least as much attention as the immiscible case: As in the immiscible case, the unfavorable viscosity ratio (displacing fluid less viscous than the displaced one) generates the instability, but here the stabilizing effect is due to the hydrodynamic dispersion which tends to spread out growing fingers. Dispersion is more subtle than interfacial tension. Furthermore, it is anisotropic and flow dependent, which leads to new predictions [6–12], such as a crossover between diffusive and linear growth regimes [7,12] and an enhancement of the instability due to the interplay of a large viscosity ratio and a velocity-dependent hydrodynamic dispersion. Experiments are scarce [1,13–18] and deal generally with a pseudo-2D geometry involving qualitative visualization. In this Letter, we use a newly developed acoustic technique to carry out the first study of the profiles of viscous fingers in 3D porous media. Our experiments have been carried out on three different porous media with a wide range of viscosity ratios and flow rates. Both the diffusive and the linear growth are observed, including the crossover from one to the other. Taken together, our data are best understood in terms of a new instability parameter that characterizes the main features of viscous fingering. Our determination of the dependence of this parameter on the viscosity ratio, on the flow rate, and on the porous medium when placed in the context of existing theory leads to new physical insights on this rich and varied problem.

We make use of the standard continuum approach [6–13], at a macroscopic scale, large compared to any details of the porous medium, and hence the equation describing mixing is a convection-dispersion formalism (CDE):

$$\frac{\partial C}{\partial t}+\mathbf{U}\cdot\nabla C=\nabla\cdot(\vec{\vec{D}}\cdot\nabla C)\,, \tag{1}$$

where $C(x,y,z,t)$ is the concentration and D is the velocity-U-dependent dispersion coefficient tensor ($D_\parallel$ in the flow direction, $D_\perp$ in the transverse direction, $\varepsilon=D_\parallel/D_\perp$). For a stable flow, a solution of (1) is a Gaussian profile [19]. Experimental determinations of concentration profiles have demonstrated [19,20] the relevance of the Gaussian dispersion statement involved in the CDE (1) and allowed the measurement of $D_\parallel(U)$.

To analyze the flow stability when a viscous fluid (viscosity μ_+) saturating the porous medium is displaced by another less-viscous fluid (μ_-) at a constant flow rate U, Eq. (1) still holds, together with fluid incompressibility and Darcy's law [7]. Miscible fluids involve a concentration-dependent viscosity $\mu(C)$. For the sake of simplicity an exponential law [$\mu(C)=\mu_-e^{RC}$] is generally assumed; extension to other laws is straightforward and will be given in a larger version [21] of this paper as well as the effects of gravity. With this set of equations one can perform either the complete calculation [11,12] of the viscous fingering process or first proceed to the physically illuminating linear stability analysis [6–10] yielding the growth rate σ of small disturbances versus their wave vector q. At time $t=0$ an analytical expression is obtained [9]:

$$2\gamma(\gamma+q)=Rq[U+L\gamma D_\parallel\tanh(\tfrac{1}{2}R)]/D_\parallel\,, \tag{2}$$

where $\gamma^2=(\sigma+D_\perp q^2)/D_\parallel$ and $L=(U/D_\parallel)(dD_\parallel/dU)$ is the exponent of the velocity-dependent hydrodynamic dispersion coefficient.

In the case $L=0$ [7] the lowest-order viscous term is destabilizing, whereas the second-order dispersion term is stabilizing, yielding a parabolic σ-vs-q curve with a maximum growth rate and a cutoff wave vector q_c.

The case $L\neq 0$ suggests a new effect [9]: For a large enough combination of both L and R, there is no cutoff wave vector q_c; all wave vectors are unstable because transverse stabilization is overcome by the destabilizating interplay of viscosity and the longitudinal dispersion velocity dependence. The crossover between the two regimes is given by the parameter η:

$$\eta=\tfrac{1}{2}LR\tanh(\tfrac{1}{2}R)-1-\sqrt{\varepsilon}\,. \tag{3}$$

For $\eta<0$, the instability is identical to the $L=0$ case; for $\eta>0$, the instability is harder [$q_c,\sigma(q_c)=\infty$]. Indeed, q

should be bounded by geometric limitation yielding a large enhancement of the growth rate at the transition ($\eta=0$); for $L=1$, $\eta=0$, for small stabilizing transverse dispersion ($\varepsilon \leq 0.1$), at $M \simeq 20$ ($R \sim 3$). Experiments are needed in this region to test the predictions.

The linear stability analysis predicts the main features at the very beginning of the instability. Further developments require one to take into account nonlinearities which allow shielding splitting and the fading of fingers [7,11,12]; numerical calculations of these basic phenomena have been performed in 2D: one of the results deals with the behavior of the overall front width Δz as fingers develop. Starting from a sharp step front at time $t=0$, its width grows first as in a diffusive process ($\Delta z \sim \sqrt{t}$), and then in a convective way ($\Delta z \sim t$): fingers spread linearly with time [13–18] as for the Saffman-Taylor instability [4].

An acoustic technique [19,20,22] is used to determine the space and time dependence of the concentration $C(z,t)$ in our samples of typical size $4\times4\times30$ cm^3. Basically, concentration measurements are derived from the velocity variations of a sound wave in ten cross sections of the sample (ten z values) with a 3-mm spatial resolution. We have previously measured [19,23] the longitudinal dispersion $D_{\parallel}$ versus the flow velocity U in a limestone (permeability $k=15\times10^{-15}$ m^2), a millstone ($k=11\times10^{-14}$ m^2), and a fireproof brick ($k=75\times10^{-12}$ m^2): As U increases, $D_{\parallel}$ increases from a molecular diffusive regime ($L=0$) to a mechanical dispersion regime ($D_{\parallel} \sim U$, $L=1$); in between, for the fireproof brick, there is an enhancement of L ($L \simeq 1.5$).

We have designed an experiment to measure $D_{\perp}$ [21]. Basically, we follow acoustically the spreading of a drop of the same density and viscosity as the fluid saturating the porous media. We go from an isotropic dispersion ($\varepsilon=1$) at low flow rate in the molecular diffusion regime (with also $L=0$) to an anisotropic regime at larger flow rate ($\varepsilon \leq 0.05$).

In the unstable flow case, the displacing fluid is pure water ($\mu_- = 8.0\times10^{-4}$ Pas at 30°C); displaced fluids are water-glycerol mixtures of different concentration, the viscosity of which varies from $\mu_+ = 8.0\times10^{-4}$ to 0.6 Pas at 30°C. From the viscosity-concentration relationship we can compute for each experiment the rescaled R and η values [21], $R=(\mu'_+ + \mu'_-)/(\mu_+ + \mu_-)$ and $L(\mu'_+ - \mu'_-)/2(\mu_+ + \mu_-) - 1 - \sqrt{\varepsilon}$, where μ values and the μ derivatives (μ') are taken at concentration $C=0$ for $-$ subscript and $C=1$ for $+$. The permeability of the samples will limit the range of available viscosity ratio and flow rate due to the large pressure drop required to flow across the sample. We note that here flows are driven vertically with gravity always as a stabilizing effect. Gravity can be of importance for the fireproof brick sample [21].

In the limestone, measurements have been possible up to $M=25$ at a flow rate ranging from 0.1 to 25 cm/h in which case $L \simeq 1$, $\varepsilon \simeq 0.05$. Figure 1(a) shows the resulting concentration profiles for $M=1.75$ ($R=0.40$) and $U=6.5$ cm/h for ten z positions ($z=2.5$, $2.5+2.1$, $2.5+4.2$ cm, . . . , from the inlet). We clearly see the instability growth as we go away from the inlet, starting with a more or less diffuse front to small growing fingers. For larger viscosity ratios the observed profiles exhibit shoulders, which is the signature of fingers [Fig. 1(b)]. In the figures we plot C versus the pore volume Ut/h (h sample length); at a given M ratio, the set of curves corresponding to different flow rate U are superimposable: The instability growth is nearly independent of the flow rate. It is obvious that experimental profiles are more unstable in Fig. 1(b) than in 1(a); however, we need a more quantitative characterization of the degree of instability. As suggested in Refs. [7,12], the profile width is characteristic of the overall instability. Since we have ten profiles at ten z values, we measure for each profile the time width between $C=0.1$ and $C=0.9$ (the exact choice of numerical values of C is arbitrary, but the result is not sensitive to the values chosen). From the stable flow measurements we also know the stable time width due to dispersion [19]. Hence we characterize each instability profile by the time excess width δt, which is the difference between the unstable and stable time widths at the same location z and flow velocity. Moreover, to take into account the flow independence, we will plot $U\delta t$ vs z as the instability characteristic. The resulting analysis of the

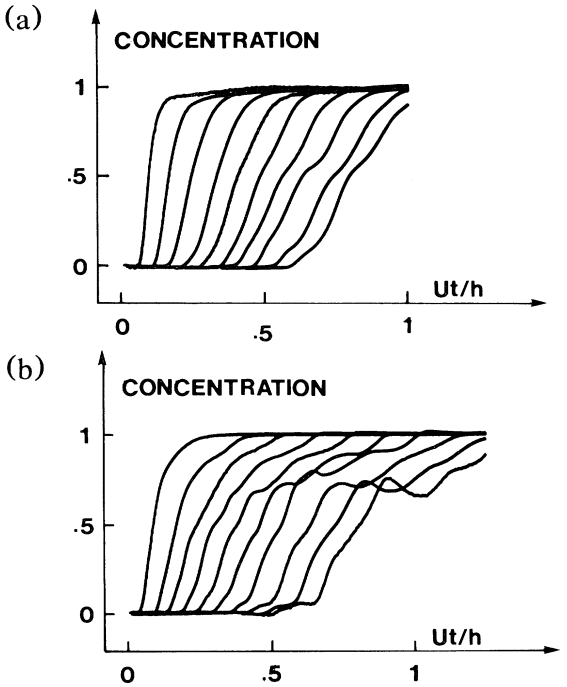

FIG. 1. Concentration profiles: concentration vs reduced time (Ut/h, h sample length) at flow rate $U=6.5$ cm/h in limestone. From left to right each profile corresponds to increasing distance z from the inlet (2.5, 2.5+2.1, 2.5+4.2 cm,...). (a) Viscosity ratio $M=1.75$. (b) $M=3.16$.

data of Figs. 1(a) and 1(b) is given in Fig. 2. For the low viscosity ratio, as can be seen from the direct profile, we do observe a crossover from a diffusive regime ($U\delta t \sim \sqrt{z}$, dash-dotted line) at low z values to the fully developed fingers regime ($U\delta t \sim z$, dashed line), whereas the large-viscosity-ratio experiment only exhibits the last regime. The low-viscosity-ratio experiment clearly demonstrates the crossover between the diffusive and the developed fingers regime in agreement with the numerical simulations [7,12]. The initial small disturbances grow, shield, and spread, leading first to an enlarged front which still looks like a diffusive front. When the disturbances become large enough, nonlinearities stabilize the fingers, which just grow further linearly with time. We emphasize that the observation of the crossover is not easy. We observe it at $M=1.75$. For $M=1.18$ the sample is not long enough to exhibit the crossover (diffusive all along the sample), whereas for $M=2.18$ instability has already developed at the shortest distance from the inlet ($z=2.5$ cm).

The linear temporal spreading of the fingers when the instability is fully settled is characterized only by the slope of $U\delta t$ vs z: We take $p=U\delta t/z$ as our experimental parameter. In the limestone, the flow independence leads to a plateau in a plot of p vs U. As the relevant effect of M in the stability analysis is through R, in Fig. 3 we give a plot of p against R: The data are nearly linear, meaning that our experimental parameter p used to describe the fingering is simply proportional to R.

In the millstone, we have studied the viscosity ratio M from 1.25 to 760. The higher viscosity ratios have been obtained at the cost of a limited range of flow rate, yielding $L\sim 0$ and $\varepsilon\sim 1$, and then $\eta<0$ always in this medium. As in the limestone, in the millstone the fingers develop with a linear time dependence of the excess width ($U\delta t \propto z$). The corresponding parameters p are given in Fig. 3; the two measurements at $M=135$ and 760 also align nicely with the others, even for different values of L and ε but still with $\eta<0$. This gives more confidence in the proportionality to R of our experimental parameter p. A larger slope of p vs R is obtained for the limestone than for the millstone, presumably because the millstone is much more homogenous than the limestone. In the millstone fluctuations of permeability are of the order of 25%, whereas for the heterogenous limestone we measure fluctuations up to 200% [24].

The fireproof brick sample is a good candidate to test the hard transition ($L\sim 1.5$), but due to its large permeability there are gravity effects. To get rid of these stabilizing effects requires much larger flow rates than the critical velocity [1,21] resulting in a limitation of the viscosity ratio to $M\sim 135$. As for the two previous samples, fingers develop with a linear time dependence. For $M<25$, the corresponding parameters p once again are linear with R (Fig. 3) with a slope close to the one of the millstone (they both have the same order of magnitude of permeability fluctuations).

For the two larger M values ($M=50$ and 135), we can only get a lower bound of p [21]. However, these data (Fig. 3) are well above the linear R relationship (especially for $M=135$). Guided by the linear stability analysis one would think that this behavior corresponds to the prediction of a harder instability for large M values [9]. To support this, we note that the conditions necessary for such a larger instability growth ($\eta>0$) are fulfilled: From R, L, and ε values, using (4), we get $\eta\sim 7$ for $M=135$ ($L=1.5$, $\varepsilon=0.1$), well above the threshold ($\eta\simeq 0$), and $\eta\sim 2.5$ for $M=50$.

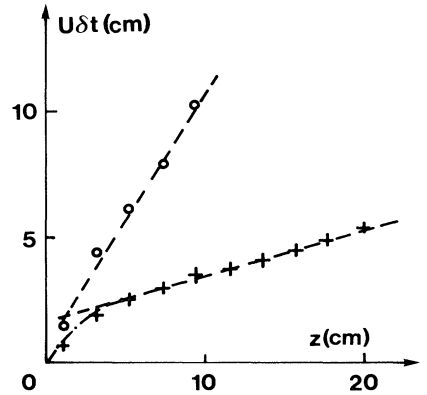

FIG. 2. Excess width ($U\delta t$) of the profile vs distance z from the inlet. + and o correspond to Figs. 1(a) and 1(b). The dash-dotted line is a guide for the eye for the diffusive regime. The dashed lines are the linear temporal spreading regime; the slope of the dashed line is our experimental parameter p.

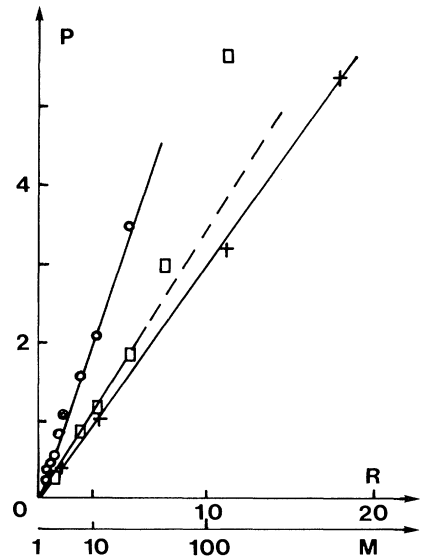

FIG. 3. Experimental parameter p vs the viscosity variable R for the limestone (o), the millstone (+), and the fireproof brick (□). M is the viscosity ratio.

Let us summarize the experimental features and compare them with the theory. (i) The crossover, observed experimentally, between a diffusive regime ($\sim\sqrt{t}$ growth) and a convective regime ($\sim t$ growth) for the width of the profile is in agreement with numerical simulations [7,12] of finger growth in a porous medium. (ii) In the convective regime, in which fingers grow linearly with time, we have been able to define an instability parameter p which characterizes the overall instability growth. (iii) In most of the cases analyzed, the only p viscosity dependence is linear with R ($R \sim \ln M$). The larger the heterogeneity of the medium, the larger the slope of p vs R. There are no corresponding predictions except that the viscosity ratio enters in the theory only through R. (iv) An enhancement of the initial growth rate under the subtle interplay of a large viscosity ratio and a velocity-dependent hydrodynamic dispersion has been predicted [9]; this is a way to account for the large-M data in the fireproof brick which are well above the $p \sim R$ relationship and for which the theoretical conditions are totally fulfilled. As we do not observe this effect in the millstone even with a larger viscosity ratio ($M = 760$), but a much lower L, these two porous media demonstrate that both large M and large L are required to obtain this effect.

Our experiment in real three-dimensional porous media yields a dependence of p on viscosity ratio and flow velocity which may stimulate further development of the theory.

This paper benefits from stimulating discussions with J. Banavar, G. M. Homsy, F. M. Orr, N. Rakotomalala, H. Tchelepi, Y. C. Yortsos, and W. Zimmermann. This work has been partly supported by NATO Grant No. 0209.1988. Laboratoire d'Acoustique et Optique de la Matière Condensée is associated with the Centre National de la Recherche Scientifique.

[1] S. Hill, Chem. Eng. Sci. **1**, 247 (1952).
[2] G. M. Homsy, Annu. Rev. Fluid Mech. **19**, 271 (1987), and references therein.
[3] Y. C. Yortsos, J. Phys. Condens. Matter **2**, SA 443 (1990), and references therein.
[4] P. G. Saffman and G. I. Taylor, Proc. Roy. Soc. London A **24**, 312 (1958).
[5] D. Bensimon, L. P. Kadanoff, S. Liang, B. I. Shraiman, and C. Tang, Rev. Mod. Phys. **58**, 977 (1986).
[6] R. A. Wooding, J. Fluid Mech. **39**, 477 (1969).
[7] C.-T. Tan and G. M. Homsy, Phys. Fluids **29**, 3549 (1986); **31**, 1330 (1988).
[8] F. J. Hickernell and Y. C. Yortsos, Stud. Appl. Math. **74**, 93 (1986).
[9] Y. C. Yortsos and M. Zeybek, Phys. Fluids **31**, 3511 (1988).
[10] Y. C. Yortsos and F. J. Hickernell, SIAM J. Appl. Math. **49**, 730 (1989).
[11] M. A. Christie (to be published).
[12] W. Zimmerman and G. M. Homsy, Phys. Fluids A (to be published).
[13] U. Araktingi and F. M. Orr, contribution No. 18095 to the SPE Annual Technical Conference and Exhibition, Houston, 1988 (unpublished), and references therein.
[14] R. J. Blackwell, J. R. Rayne, and W. M. Terry, Trans. Metall. Soc. AIME **216**, 1 (1959).
[15] B. Habermann, Trans. Metall. Soc. AIME **219**, 264 (1960).
[16] R. L. Slobod and R. A. Thomas, Soc. Pet. Eng. J. **3**, 9 (1963).
[17] R. L. Perkin, O. C. Johnston, and R. N. Hoffman, Soc. Pet. Eng. J. **5**, 301 (1965).
[18] J.-C. Bacri, N. Rakotomalala, and D. Salin, *Physics and Chemistry of Porous Media* (AIP, New York, 1987).
[19] J.-C. Bacri, N. Rakotomalala, and D. Salin, Phys. Fluids A **2**, 674 (1990).
[20] J.-C. Bacri, N. Rakotomalala, and D. Salin, Phys. Rev. Lett. **58**, 2035 (1987).
[21] J.-C. Bacri, D. Salin, and R. Wouméni (to be published).
[22] J.-C. Bacri, M. Hoyos, N. Rakotomalala, D. Salin, M. Bourlion, R. Lenormand, and A. Soucemarianadin, J. Phys. (Paris) **1**, 1455 (1991).
[23] J.-P. Hulin and D. Salin, in *Disorder and Mixing,* edited by E. Guyon, J.-P. Nadal, and Y. Pomeau, NATO Advanced Study Institutes, Ser. E, Vol. 152 (Plenum, New York, 1988), p. 89.
[24] H. Tchelepi (private communication).